Mechanical Properties Evaluation of Coir Toughened Unsaturated Polyester with Different Reinforced Body Forms

Jia Yao,[a] Wei Lu,[a] Shoufan Rong,[b] and Yingcheng Hu [c,]*

Unsaturated polyester (UPE) composites reinforced with natural fiber as non-structural materials have been used in engineering. In this study, three different types of coir-reinforced UPE consisting of coir non-woven needle mat (CNM), coir mesh (CM), and coir rope (CR) were produced, and the mechanical properties, such as flexural strength (FS), tensile strength (TS), and impact toughness (IT), were investigated. With the exception of FS, CR-reinforced UPE composites exhibited better mechanical properties, mainly due to good directionality of the coir fibers. Dynamic mechanical analysis (DMA) was also carried out to analyze the composite performances under wide temperature ranges. All the tests confirmed the beneficial effect of coir on the UPE matrix, noting that composites with higher toughness perform better in most applications.

Keywords: Coir; Unsaturated polyester; Reinforced body forms; Impacting toughness; Dynamic mechanical analysis (DMA)

Contact information: a: College of Mechanical Engineering, Jiamusi University, 154007, Jiamusi, China; b: College of Material Engineering, Jiamusi University, 154007, Jiamusi, China; c: Key Laboratory of Bio-based Material Science and Technology of Ministry of Education of China, College of Material Science and Engineering, Northeast Forestry University, Harbin,150040, China;
** Corresponding author: yingchenghu@163.com*

INTRODUCTION

Since the beginning of the last century, composites reinforced with fiber have been developed for diverse applications, such as packing materials, aerospace components, and automobile materials. This is largely due to the utilization of glass, carbon, or aramid fibers reinforcing the epoxy, UPE resins, polyurethanes, or phenolics. Good industrial ecology, high efficiency energy production, and green chemistry are motivations for the development of the next generation of composite materials. Fiber-reinforced plastic composites were first developed by combining natural fibers with phenolic resin in 1908. Natural fiber reinforced composites are initially aimed at the replacement of glass fiber reinforced composites because natural fibers are not only cheaper than glass fibers but also cause less health problems for people (Joshi *et al.* 2004).

The thermosets constitute the majority of resins used in the composite industry. Among various thermoset resins, UPEs are the most widely used matrix materials in polymeric composites because of their relatively low price, low density, ease of handling, thermal and dimensional stability, and excellent mechanical properties. Furthermore, compared to other thermoset polyesters, UPEs can easily achieve fiber reinforcement in a liquid form. In recent years, the uses of natural fibers as reinforcement in UPE have been described in many publications. Venkata Reddy *et al.* (2008, 2009) studied the impact properties of kapok-based UPE hybrid composites. Hughes *et al*. (1999) found that non-woven hemp-reinforced UPE composites exhibited higher toughness than short-cut glass fiber-reinforced UPE composites. Sèbe *et al*. (2000) examined the FS and flexural modulus of non-woven hemp fiber mat-reinforced UPE composites, which was produced using resin transfer moulding; the properties increased when the fiber contents were increased in the range 0 to 36 wt.%. Jani and Kumar (1996) found that the strength of bamboo-reinforced UPE composites was better than that of glass fiber-reinforced UPE composites. O'Dell (1997) used non-woven jute fibers to prepare UPE panels and found that TS, tensile modulus, and flexural modulus of the jute specimens were half the values of the glass fiber-reinforced UPE composites; IT and TS were also lower. The comparison of sisal, jute, flax, and glass fiber-reinforced UPE composites has been carried out, and the results suggested that among the three natural fibers reinforced composites, the jute-reinforced UPE composites exhibited the best FS and TS, and the worst IT (Rodríguez *et al.* 2005; Udaya Kiran *et al.* 2007). In another investigation, Hill and Abdul Khalil (2000) have used non-woven mats of random coir and oil palm fibers (0 to 55 wt.%) to reinforce UPE using compression moulding, and FS values of all the composites were found to be lower than those for plain UPE at all fiber contents. Lai *et al*. (2008) reported woven betel palm and kenaf lignocellulosic fibers as a reinforcing phase in unsaturated polyester. Abrala *et al.* (2012) have studied the effects of alkali treatments for various soaking time and the effect of fiber content on mechanical properties of *Pandanus odoratissimus* fibers-reinforced unsaturated polyester matrix composites. According to the above results, the advantages of natural fiber-reinforced UPE are the realization of the reduced production cost as well as the lowered weight.

Coir is a natural fiber with excellent impact toughness because it has the highest elongation at break and the largest micro-fibrillar angle (Saravana Bavan and Mohan Kumar 2010). Therefore, coir has been judged to be the best suitable fiber for the toughened optimal design of composites (Yao *et al.* 2011). Coir-reinforced UPE composites used for helmets, roofing materials, and post boxes materials have also been investigated (Jayabal and Natarajan 2011). In order to optimize the properties of UPE composites, different coir-reinforced forms were adopted to change the load bearing characteristics under the different loading states. In the present work, three different coir-reinforced body forms including coir non-woven needle mat (CNM), coir mesh (CM), and coir rope (CR) were used. The influences of different reinforced forms and the contents of coir on the performance of the coir reinforced UPE composites were analyzed. The dynamic mechanical performance evaluations have been done by DMA, and the surface morphologies of the specimens have been investigated using environment scanning electron microscopy (ESEM).

EXPERIMENTAL

Materials

Among the three reinforced forms of coir using in this research, CNM and CR were bought from Juxin Coconut Palm Products Co. Ltd, Weifang, Shandong province of China, but CM was woven by hand using CR. The density of CNM was 1.2 g/cm^3. In all the three coir-reinforced forms, the orientations of the fibers in different reinforced forms are chaotic, unidirectional, and bidirectional, respectively. The coarseness of CR was 0.3

cm, and the weight per meter of CR was 7 g. The amount of added CM can be adjusted according to the mesh size. Before the composite material preparation, these three reinforced forms of coir were first dried at 120 °C for 10 h to maintain water content less than 5 wt.% in order to enhance the interface adhesion quality (Moraes *et al.* 2003). UPE TM-196SP (from Changzhou Huari New Material Co., Ltd of China) was used as matrix. In order to accelerate the curing of the matrix resins at room temperature, butanox M-50, methyl ethyl ketone peroxide, and cobalt naphthenate were used as hardener, accelerator, and catalyst, respectively.

Composite Preparation

Coir raw materials of three types were first pre-impregnated into the matrix material consisting of UPE resin to ensure the full dip of coir fibers. A hand-lay-up method was adopted to fill up the prepared semi-open mold using UPE resin with 2 wt.% hardener, 1 wt.% accelerator, and 1 wt.% catalyst added into UPE resin at room temperature by the weight of each resin. Also, the weight percent content (WPC) of CNM, CR, and CM forms were 10 wt.%, 15 wt.%, 20 wt.%, 25 wt.%, or 30 wt.%, as shown in Table 1.

Table 1. Experimental Design and Mechanical Properties

Specimen number	Reinforced body forms	WPC （wt%）	FS (MPa)	TS （MPa）	IT (kJ/m^2)
1	CNM	10	26.54	18.72	3.62
2	CNM	15	30.02	20.20	5.56
3	CNM	20	38.97	24.97	8.26
4	CNM	25	39.24	21.34	9.55
5	CNM	30	35.51	20.94	10.82
6	CM	10	39.84	13.70	8.87
7	CM	15	43.67	15.02	12.45
8	CM	20	49.98	17.56	18.30
9	CM	25	51.25	19.67	21.32
10	CM	30	53.65	22.30	25.78
11	CR	10	41.83	16.53	13.12
12	CR	15	42.67	18.3	16.49
13	CR	20	43.07	23.41	19.12
14	CR	25	45.68	25.03	23.87
15	CR	30	47.53	26.31	27.45
16	Plain UPE	0	49.00	29.90	8.44

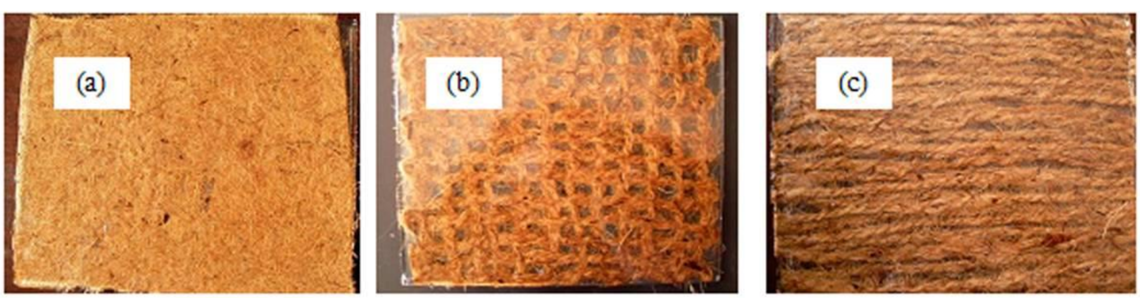

Fig. 1. Morphologies of three reinforced forms:
(a) CNM-reinforced UPE, (b) CR-reinforced UPE, (c) CM-reinforced UPE

The highest content limit of 30 wt.% coir was due to the consideration of the effect of packing degree of coir. For comparison, preparation and properties of plain UPE without coir were also performed under the same conditions. During the curing process, a compression pressure of 0.05 MPa was applied using dead weights on the mold for 1 h, and the composite specimens were removed from the mold and cured at room temperature for 24 h. Representative morphologies of three reinforced forms are shown in Fig. 1.

Mechanical Properties Testing

Tensile strength and flexural strength were determined using a RGT-20A microcomputer-controlled electronic universal test machine (made by Shenzhen Ruigeir Instrument Co., LTD of China). The specimen size for the FS test and the TS test was 100 mm×15 mm×4 mm and 180 mm×10 mm×4 mm, respectively. FS and TS were determined according to ISO 14125:1998 and ISO 527-4:1997, respectively. IT of the specimens with size 80 mm×10 mm×4 mm was measured using a XJ-50 Z type combined impact toughness test machine according to ISO 527-4:1997. All tests were carried out at 25 °C and a relative humidity of 50%. For statistical purposes, the values were mathematically averaged, and they were obtained from five replicate specimens. After the mechanical experiment, the observations of fracture surface were carried out using a Quanta 200 type ESEM (made by FEI Company of USA). Before ESEM observation, the specimen surfaces were sputter-coated with gold to avoid charging.

Dynamic Mechanical Properties

Dynamic mechanical properties of the resin and composites were measured using a DMA-242C(NETZSCH) type machine under three-point bending tests. The dimensions of the specimens were 50 mm ×10 mm × 3 mm. Temperature ranges were -20 ^{o}C to +200 ^{o}C, and the heating rate was set at 5 ^{o}C/min.

RESULTS AND DISCUSSION

The average values of FS, TS, and IT of different reinforced body forms are presented in Table 1. From Table 1, it can be seen that not only the inner structures of reinforced body forms, but also the coir content, can significantly influence the properties of the composites under different loads, as addressed below.

Comparison Analysis of FS

Figure 2 shows FS as a function of coir contents in different coir-reinforced body forms. Clearly, the FS of three reinforced composites exhibited different changing tendencies with the increasing of coir content. For both CM- and CR-reinforced composites, FS increased with the increasing of coir content. However, the FS values of CNM reinforced composites first increased from 26.54 MPa to 39.24 MPa with the coir content increasing from 10 wt.% to 25 wt.% and then decreased to 35.51 MPa when the coir content was 30 wt.%. From the comparison in Fig. 2, it can also be seen that both CM- and CR-reinforced composites exhibited a comparable FS at 10 wt.% coir content; however, CM-reinforced composites exhibited higher FS values when the coir content was larger than 15 wt.%. At all coir contents, CNM-reinforced composites exhibited the lowest FS values.

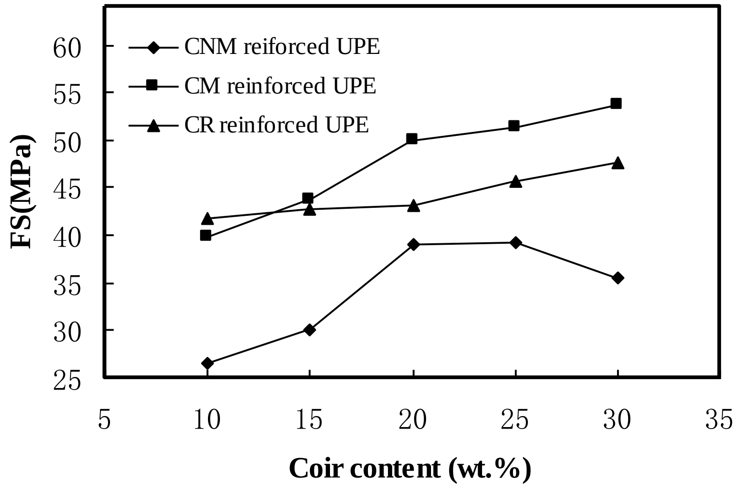

Fig. 2. Relationship of FS plotted as a function of coir content

When the coir content in the CNM-reinforced composites was low, the coir fibers exhibited a discontinuous distribution in the inner of UPE matrix, which was like the existing impurities, and relatively lower mechanical performance was observed. The CNM component, which has a certain strength on its own, can bear the loads together with UPE matrix when subjected to the bending load, so FS increased with the increasing of coir content. With the further increasing of coir fibers to 30 wt.%, UPE resins were not enough to realize better adhesion with coir, and a weak internal interface adhesion became apparent. Cracks occurred easily under the bending loads, leading to the reduction of material mechanical properties. However, FS increased linearly with the increasing of coir content for the other two reinforced body forms. This was attributed to the interweaving function of CRs, forming a two-dimensional constraint structure in the CM structure, which was very effective in resisting the bending loads. When the coir content was 20 wt.%, the values of FS- of CM-reinforced UPE exceeded that of the plain UPE of 49 MPa; when the coir content increased to 30 wt.%, a higher FS of 53.65 MPa was observed compared to that of the plain UPE.

For CR, its form was equivalent to adding reinforced steel bar in the cement matrix; therefore a higher FS was observed compared with CNM. However, ropes do not have the mutual constraint function as in a CM structure, so FS values of CR-reinforced UPE were lower than the plain UPE. From the above results, it could be found that CM exhibited the best reinforcing effect, leading to increases in the FS in the three types of coir-reinforced body forms.

Comparison Analysis of TS

Figure 3 shows TS as a function of coir contents in different coir-reinforced body forms. Clearly, the values of TS of three reinforced composites also exhibited different changing tendency with the increasing of coir content. For both CM- and CR-reinforced composites, the values of TS increased with the increase of coir content. However, the TS for CNM first increased from 18.72 MPa to 24.97 MPa with the coir content changing from 10 wt.% to 20 wt.% and then decreased to 21.34 MPa when the coir content was 25 wt.%, and further decreased to 20.94 MPa when the coir content was 30 wt.%.

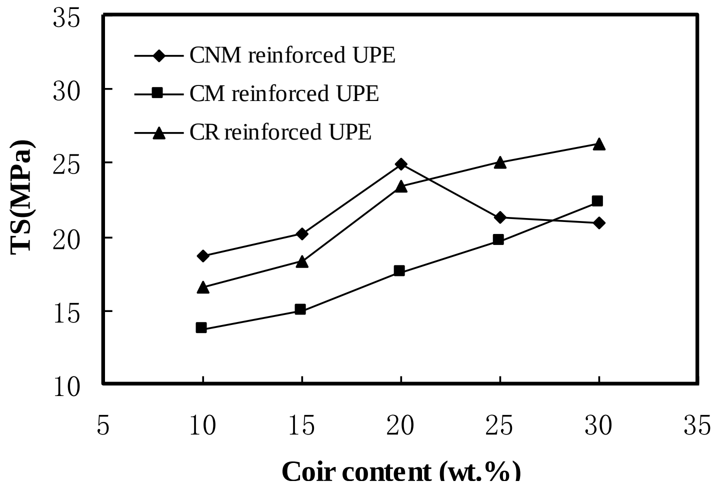

Fig. 3. Relationship of TS plotted as a function of coir content

Based on the comparison in Fig. 3, it can be noted that among the three reinforced types composites, when coir content was less than 20 wt.%, the values of TS for CNM-reinforced composites were the highest. This suggests that the tensile load capacity mainly stems from UPE matrix. Lower coir content would have large destructive effects on the matrix for CR- and CM-reinforced composites; when it was increased to 30 wt.%, the tensile load function of CR- and CM-reinforced composites will exceed that of CNM-reinforced composites. For CNM-reinforced composites, the values of TS within this research first increased and then decreased, which could be explained in a similar way, as in the case of FS, as addressed above. With the increasing of coir content, the values of TS showed an obvious increasing tendency for two other reinforced body forms. The main reason was that the fiber distribution direction in CR was consistent with the tensile loads, so the resistant ability of tensile loads was stronger. For CM-reinforced composites, the fiber distribution directions were in two directions, one being consistent with the tensile load, and the other vertical to the tensile load. So at the same coir content, CM-reinforced composite exhibited lower TS than that of CR-reinforced composites.

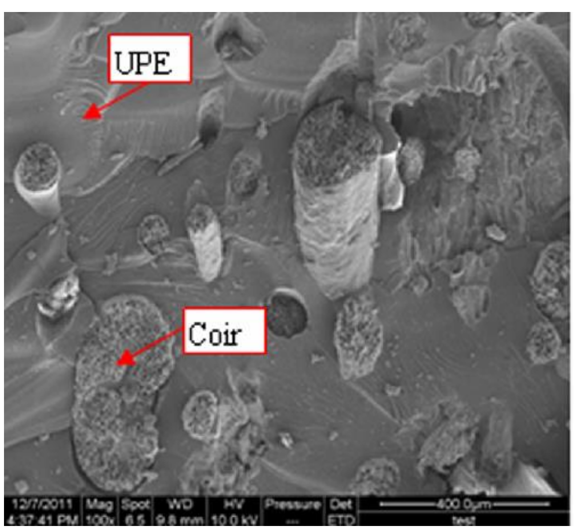

Fig. 4. Fracture surfaces of CR-reinforced specimens after tensile strength test

Figure 4 shows a representative fracture surface morphology of CR-reinforced composites after tensile strength testing. Clearly, there existed many forms of damage of the coir in CR-reinforced specimens when suffering tensile damaging loads. Forms of damage mainly involves pull-out of coir and fracture of coir. There was also a necking phenomenon of coir under the tensile loads, which made the tensile fracture more difficult. The comprehensive damaging forms of coir make the tensile damage more difficult for the higher coir content in the CR forms.

Comparison Analysis of IT

Figure 5 shows IT as a function of coir contents in different coir-reinforced body forms. Clearly, a similar increasing tendency of IT in three reinforced composites with the increasing of coir content was observed. From Table 1 and Fig. 6, it can be found that the addition of coir fibers significantly enhanced the IT of the composites following the order of CR＞CM＞CNM. When the coir content exceeded 20 wt.%, the values of IT of CNM-reinforced composites were almost equal to that of the plain UPE. For the other two reinforced body forms, the values of IT were equal to or higher than that of the plain UPE even containing about 10 wt.% coir, as shown in Table 1. The phenomena were relevant to the different inner structures of reinforced body forms, as addressed below. For CNM-reinforced composites, the mutual restrictions among fibers were limited due to the random distribution of coir fibers, which caused a weak load bearing ability for the horizontal load to fibers in the impact period.

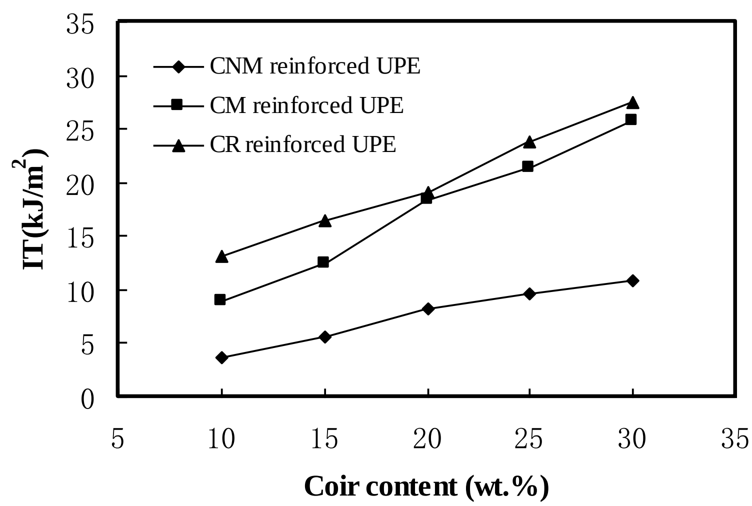

Fig. 5. Relationship of IT plotted as a function of coir content

For CM-reinforced composites, the vertical and horizontal interweaving of ropes formed a large amount of net meshes, and these could be filled with the relatively brittle UPE matrix. Impact cracks were more likely to appear and expand in the inner meshes during the impaction test. For CR-reinforced composite, as discussed above, the whole CR can be regarded as a continuous unidirectional fiber to resist impact loads. The impact damage for the whole composite can be realized by first destroying the winding structure of fiber ropes and then destroying the great quantities of coir fibers in the impact section. The total energy consumption during the impacting test was much greater for CR-reinforced UPE. Although fiber ropes amounts for CM and CR were equal at the same coir content, the impact load absorption abilities varied greatly due to the different fiber ropes distribution in terms of direction. The IT values of CR-reinforced UPE were always more than that of CM-reinforced UPE under the same coir content as in Fig. 5.

Figure 6 shows representative fracture surface morphologies of CR-reinforced composites after an impact test. The impact energy absorption mainly resulted from fiber breakage, coir pull-out, fiber de-bonding, and fiber micro-fibrillation, as in Fig. 6(a). The micro-fibril angle of coir was the largest in all plant fibers, so the micro-fibrillation was regarded as the main means of energy consumption. From Fig. 6(b), it can be found that the UPE penetrated into the cell lumen of coir. Therefore, the coir itself and the UPE in the fiber cells can play a joint role in dissipating the impact energy under the impact load. The above results can be used to explain the higher impact toughness of coir-toughened UPE composites based on a microscopic damage theory.

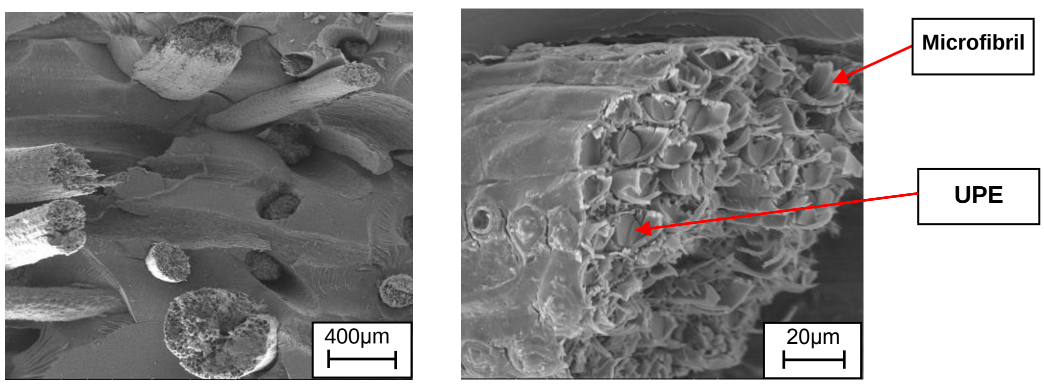

(a) (b)

Fig. 6. Fracture surfaces of CR reinforced specimens after impacting test

DMA

Dynamic mechanical test methods have been widely employed for investigating the structures and viscoelastic behavior of polymeric materials in order to determine their relevant stiffness and damping characteristics (Li 2008). The dynamic properties of polymeric materials compared with static properties are of considerable practical significance to determine the glassy transition state temperature (T_g) and the energy absorbing ability in cyclic loads. The DMA of 20 wt.% and 30 wt.% CR-reinforced composites, 30 wt.% CNM-reinforced composites, and plain UPE were studied in detail.

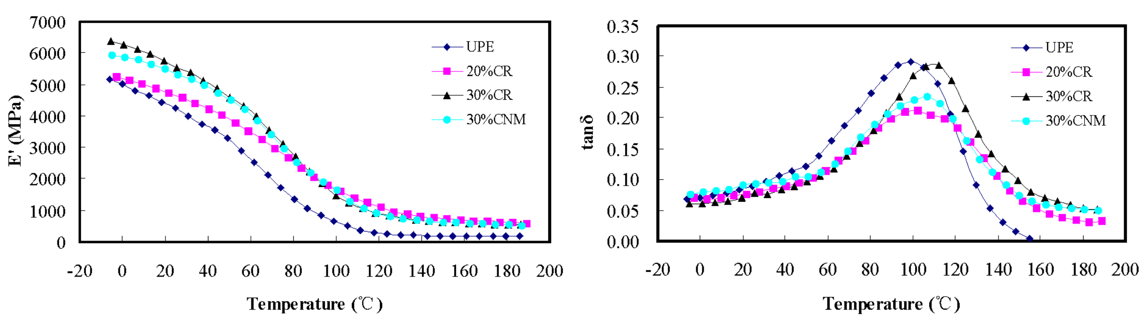

(a) (b)

Fig. 7. Modulus of energy storage (E') and Mechanical loss ($\tan\delta$)

Figure 7(a) shows the modulus of energy storage (*E'*) as a function of temperature of different specimens. Clearly, a different variation of modulus of energy storage was observed due to the different effect of the incorporated coir fibers. For the plain UPE, the values of *E'* was the smallest of the four specimens. It is important to mention that the modulus in the glassy state is determined primarily by the strength of the intermolecular forces and the way the polymer chains is packed (Klemm *et al.* 1998). The 30 wt.% CR- and 30 wt.% CNM-reinforced composites almost had comparable E' values at temperatures higher than the glass transition temperature T_g. However, the reduction of the modulus for 20 wt.% CR-reinforced composites during heating to the glass transition temperature was the smallest due to better interfaces between the coir fibers and UPE matrix, which resulted in higher E' values at temperatures higher than 100 °C.

Mechanical loss (tan δ) is a damping term that can be related to the impact resistance of a material. The damping peak occurs at the region of the glass transition temperature where the material changes from a rigid to a more elastic state, as seen in Fig. 7(b); this is associated with the movement of small groups and chains of molecules within the polymer structure. In a composite system, the incorporation of fibers signifycantly affected the damping. The composite mixture law can predict the basic mechanical properties of composites; it also can be used to predict the material buffering characteristics (Nielsen 1974). Composite damping properties result from the inherent damping of the constituents (Dong and Gauvin 1993) according to Eq. (1):

$$\tan\delta_c = V_f \tan\delta_f + (1 - V_f)\tan\delta_m \qquad (1)$$

where tan δ_c, tan δ_f, and tan δ_f are the damping values of the composite, the fiber, and the polymer, respectively. The parameter V_f is the volume fraction of the fiber.

The damping ability of coir was superior to that of the matrix resin, as discussed in IT analysis for the coir-reinforced UPE composites. The total damping ability of coir-reinforced UPE composites increased according to the Eq. (1) due to the increasing of coir volume content, as shown in Fig. 7(b).

The width of the tan δ peak of coir-reinforced UPE also became broader compared to the UPE matrix. These results suggest that there existed molecular relaxations in the composites that were not present in the plain UPE matrix. Molecular motions at the interfacial region generally contribute to the damping of the material apart from those of the constituents. Hence the width of the tan δ peak is indicative of the increased volume of the interface. The concentration of the fibers increases the interface (Landel 1994).

Stress-induced motions may also occur in the composite. The hydrogen bonds between coir and the matrix may break under stress. After such a break, a small amount of molecular motion can occur, which makes it difficult for the same bond to reform again. As a result, a new hydrogen bond forms, which initially carries little, if any stress. As a consequence, energy dissipation and mechanical damping occurred (Murayama 1978), and CR-toughened UPE with 30 wt.% coir had the highest toughness under the DMA condition. The above DMA results indicated that the coir-toughened composites can be used over a wide range of temperatures. The buffer performance of coir-toughened UPE composites was excellent.

CONCLUSIONS

1. In this research, three different types of coir fiber-reinforced unsaturated polyester (UPE), consisting of coir non-woven needle mat (CNM), coir mesh (CM), and coir rope (CR) were designed, and their mechanical properties were investigated. The three different types of reinforced composite exhibited different trends of changes in flexural strength (FS) and tensile strength (TS) values with the increasing of coir content due to the completely different inner structures for the three reinforced forms. For the three reinforced body forms, a linearly increasing trend occurred for impact toughness (IT), and the reinforced effect order for IT was CR＞CM＞CNM. CR-reinforced UPE composites exhibited better mechanical properties, with the exception of FS, mainly due to good directionality. DMA results showed that 30 wt.% CR-reinforced UPE exhibited higher modulus of energy storage and better damping ability under high temperature conditions.
2. Using different reinforced body forms of plant fibers can be used as a new design idea to obtain better comprehensive performance of composites. The designed coir-toughened UPE composites can be used to resist impacting load more effectively. This research has demonstrated the optimization design of different coir-reinforced body forms to reinforce the UPE matrix.

ACKNOWLEDGMENTS

This project was funded by National Natural Science Foundation of China (51203061, 31010103905, 31170516), and the Fundamental Research Funds for the Central Universities (DL12EB03).

REFERENCES CITED

Abrala, H., Andriyantoa, H., Sameraa, R., Sapuan, S. M., and Ishak, M. R. (2012). "Mechanical properties of screw pine (*Pandanus odoratissimus*) fibers-unsaturated polyester composites," *Polym. Plastics Technol. Eng*. 51(5), 500-506.

Dong, S., and Gauvin, R. (1993). "Application of dynamic mechanical analysis for the study of the interfacial region in carbon fiber/epoxy composite materials," *Poly. Comp*. 14, 414-420.

Hill, C. A. S., and Abdul Khalil, H. P. S. (2000). "Effect of fiber treatments on mechanical properties of coir or oil palm fiber reinforced polyester composites," *J. Appl. Polym. Sci*. 78, 1685-1697.

Hughes, M., Mott, L., and Hague, J. (1999). "The toughness of vegetable fiber-reinforced upe composites," Fifth international conference on wood fiberastic composites, 175-184.

Jani, S., and Kumar, R. (1996). "Mechanical behaviour of bamboo fibers reinforced plastic (BFRP) composite and effect of environment on properties," *Processing and Fabrication of Advanced Materials* 5, 443-456.

Jayabal, S., and Natarajan, U. (2011). "Influence of fiber parameters on tensile, flexural, and impact properties of nonwoven coir-polyester composites," *Int. J. Adv. Manuf. Technol*. 54(5-8), 639-648.

Joshi, S. V., Drzal, L. T., Mohanty, A. K., and Arora, S. (2004). "Are natural fiber composites environmentally superior to glass fiber reinforced composites?" *Composites: Part A* 35(3), 371-376.

Klemm, D., Philipp, B., Heinze, T., Heinze, U., and Wagenknecht, W. (1998). *Comprehensive Cellulose Chemistry*, Wiley–VCH.

Lai, W. L., Mariatt, M. I., and Mohamad Jani, S. (2008). "The properties of woven kenaf and betel palm (*Areca catechu*) reinforced unsaturated polyester composites," *Polym. Plastics Technol. Eng*. 47, 1193-1199.

Landel, R. F. (1994). *Mechanical Properties of Polymers and Composites,* Marcel Dekker, Inc., New York.

Li, J. (2008). *Biomass Material Science*, Science Technology Press, China.

Moraes, G. S., Alsina, O. L. D., and Carvalho, L. H. (2003). "Water sorption effects on the mechanical properties of polyester-vegetable fiber composites," In: 7th Annual Brazilian Congress of Polymers. Brazil: Organized by the Brazilian polymers Association, 1062-1064.

Murayama, T. (1978). *Dynamic Mechanical Analysis of Polymeric Materials*, 2nd Ed., Elsevier, Amsterdam.

Nielsen, L. E. (1974). *Mechanical Properties of Polymers and Composites*, Marcel Dekker, New York.

O'Dell, J. L. (1997). "Natural fibers in resin transfer molded composites," Fourth International Conference on Woodfiber-Plastic Composites, 280-285.

Rodríguez, E., Petrucci, R., Puglia, D., Kenny, J. M., and Vázquez, A. (2005). "Characterization of composites based on natural and glass fibers obtained by vacuum infusion," *J. Comp. Mater*. 39(3), 265-282.

Saravana Bavan, D., and Mohan Kumar, G. C. (2010). "Potential use of natural fiber composite materials in India," *J. Reinf. Plast. Compos*. 29(24), 3600-3613.

Sebe, G., Cetin, N. S., Hill, C. A. S., and Hughes, M. (2000). "RTM hemp fiber - reinforced polyester composites,"*Appl. Compos. Mater*. 7, 341-349.

Udaya Kiran, C., Ramachandra Reddy, G., Dabade, B. M., and Rajesham, S. (2007). "Tensile properties of sun hemp, banana and sisal fiber reinforced polyester composites," *J. Reinf. Plast. Compos*. 26(10), 1043-1050.

Venkata Reddy, G., Noorunnisa Khanam, P., and Shobha Rani, T. (2009). "Flexural, compressive, and interlaminar shear strength properties of kapok/glass composites," *J. Reinf. Plast. Compos*. 28(14), 1665-1677.

Venkata Reddy, G., Shobha Rani, T., Chowdoji Rao, K., and Venkata Naidu, S. (2008). "Impact properties of kapok based UPE hybrid composites," *J. Reinf. Plast. Compos*. 27(16-17), 1789-1804.

Yao, J., Hu Y. C., and Lu W. (2011). "A wood replacement material of sandwich structure using coir fiber mats and fiberglass fabrics as core layer," *BioResources* 7(1), 663-674.

Article submitted: March 29, 2013; Peer review completed: April 29, 2013; Revised version received and accepted: May 5, 2013; Published: May 9, 2013.